Improved Reference Orbits for the Repeat-Ground-Track Missions EnMAP and Tandem-L

By Ralph Kahle,[1)] Sofya Spiridonova,[1)] and Michael Kirschner [1)]

[1)] *German Space Operations Center (DLR/GSOC), 82234 Wessling, Germany, ralph.kahle@dlr.de*

(Received April 12th, 2017)

The reference orbit implemented for the active TerraSAR-X mission works remarkably well for orbit control purposes, but an unexpected secular drift in the along-track separation between satellite and reference orbits has built up to a 60 s flight-time offset within 10 years of operation. The scope of this work is to understand the origin of the drift and to eliminate the effect for DLR's future repeat ground-track missions EnMAP and Tandem-L. The improved process of reference orbit generation is discussed and the underlying relations for the suggested inclination adjustment are derived. The improved process is successfully validated by means of 1-year numerical orbit control simulation. The presented process is generic and can be applied to any repeat-ground track mission.

Key Words: Repeat ground track, Reference orbit, Orbit dynamics, Mission analysis

Nomenclature

a	:	semi-major axis
e	:	eccentricity
i	:	inclination
J_2	:	geopotential 2nd zonal harmonic
M	:	mean anomaly
n	:	mean motion
R_E	:	Earth's equatorial radius
u	:	mean argument of latitude
μ	:	Earth's standard gravitational parameter
ω	:	argument of perigee
ω_E	:	angular velocity of Earth's rotation
Ω	:	right ascension of the ascending node

Subscripts

AN	:	ascending node
Sat	:	satellite orbit
Ref	:	reference orbit

1. Introduction

DLR's German Space Operations Center prepares for two upcoming Earth observation missions: EnMAP with a hyperspectral instrument for environmental mapping and Tandem-L – a formation flying mission with L-Band radar – aiming on the global observation of dynamic processes on the Earth's surface. Apart from the different payloads, these missions and the flying TerraSAR-X satellite (TSX) have the usage of a reference orbit in common. Such an orbit can be formulated for any Sun-synchronous repeat-ground-track mission and is typically applied for orbit control and instrument planning purposes.

This paper is motivated by a phenomenon that we are observing since the early operations phase of TSX. The TSX orbit is controlled to stay within a 250 m radius tube surrounding the Earth-fixed reference orbit (Ref), while the along-track motion is not controlled.[1, 2)] The variation of the TSX-Ref along-track distance in-between two drag make-up maneuvers is typically below ±10 km for periods of moderate solar activity as depicted in Fig. 1. However, the fall back and catch up phases are not always symmetric, building up to an oscillation with one-year period and an overlaid secular drift. After almost 10 years in orbit an along-track distance of -450 km between satellite and reference orbit has been accumulated, which corresponds to 60 s of flight time and hence change in the ascending node crossing time.

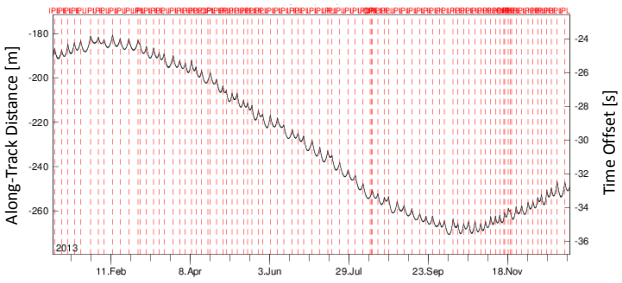

Fig. 1. Flown TSX-Ref along-track distance (left) and corresponding time off-set (right) in year 2013. Vertical red lines indicate orbit control maneuvers.

The sinusoidal behavior of the Sat-Ref along-track distance in Fig. 1 follows from the luni-solar perturbation of the orbit's inclination and RAAN. Its amplitude might be reduced by lowering the control band for the relative inclination, which however would drastically increase the number of required out-of-plane maneuvers. But, the secular variation goes back to an inclination offset on the order of 0.001° in the reference orbit. Treating this finding in the reference orbit generation

process, the secular effect can be eliminated for future repeat-ground track missions.

The paper is organized as follows. In Sect. 2 the reference orbit characteristics for three different missions and the generation process are described. Then, the long-term stability in the presence of a full perturbation environment is analyzed in Sect. 3, and the sensitivity to inclination changes is investigated in Sect. 4. The concept of applying a tiny inclination adjustment to the reference orbit ephemeris is outlined and validated in Sect. 5 and conclusions are given in Sect. 6.

2. Reference orbit characteristics and generation process

In this paper the term "reference orbit" refers to a target ephemeris for a Sun-synchronous [1], minimum altitude variation[2], repeat-ground-track[3] low-Earth orbit.

The reference orbit must be a closed orbit with matching states at the beginning and end of the repeat cycle. The reference orbit ephemeris is expressed in the Earth-fixed frame ITRF2000. In general such a reference ephemeris is valid throughout the mission duration. A simple mapping of the time axis by a rational multiple of the repeat cycle relates the reference ephemeris to any past or future period. These features make it easy to use in orbit control as well as mission planning systems.

For the reference orbit optimization process only a few mission-specific parameters have to be specified: the repeat period and number of orbits per repeat cycle, the Mean Local Time of the Ascending Node (MLTAN), and geographic longitude, latitude and date of a ground-track point that shall be part of the reference orbit, e.g. the launcher separation point or any other reference point. Apart from the reference point information, which is not relevant for this study, the necessary parameters for all three missions are given in Table 1.

Table 1. Mission orbit characteristics.

	TerraSAR-X	EnMAP	Tandem-L
Repeat period	11 days	27 days	16 days
Orbits / repeat cycle	167 orbits	398 orbits	231 orbits
Orbits / day	15 + 2/11	14 + 20/27	14 + 7/16
MLTAN	18:00	23:00	18:00

The previous process of reference orbit generation is discussed in Ref. 1) and briefly summarized in the following. It is important to point out that solely the Earth gravitational field is considered within all numerical orbit propagation steps. All other orbit perturbations (third body and tidal gravitation, irregularities of the earth's rotation, air drag and solar radiation pressure) are disabled because their impact on the orbit varies from repeat cycle to repeat cycle. By disabling these perturbations we eliminate any seasonal variation in the reference orbit. Of course, when analyzing the stability of the found reference orbit all these perturbations have to be taken into account.

As first guess the reference semi-major axis a and inclination i are derived from the desired nodal period and the regression of the right ascension of the ascending node $d\Omega/dt$ that follows from the Sun-synchronicity, respectively. For an initially circular orbit (eccentricity $e=0$) the remaining orbital elements are then found from the specified ground-track point and MLTAN. The elements a and i are iteratively adjusted and propagated over a repeat cycle by means of a Simplified General Perturbations 4 (SGP4) numerical propagator until a closed orbit is achieved.

After the first guess step a precise Earth gravity model, typically with degree and order 60, is used in order to realistically model the reference orbit. The first guess elements a and i are varied to meet the same osculating longitude and latitude after one repeat cycle. Then, the frozen orbit eccentricity is optimized following the strategy by Rosengren in Ref. 3).

At this point the numerical integration of the reference orbit over one repeat cycle typically yields ITRF2000 position differences in the order of 10 m (3d). In order to meet exactly the same state vector in the Earth-fixed frame after one cycle, a non-linear optimization problem was defined in Ref. 1) and solved by tuning a small number of virtual orbit maneuvers spread over the reference orbit. For TSX, two maneuvers with sizes of few cm/s were implemented.

Within our improved reference orbit process, closed reference orbits are obtained by varying slightly the initial Keplerian state, so that the final position and velocity vector in the ITRF2000 reference frame meets the initial one. For the direct optimization of the initial state, the General Environment for Simulation and Optimization (GESOP) software is used.[4)] While GESOP provides the optimization, simulation and plotting environment, a model has to be provided for every specific optimization problem including its particular differential equations, boundary conditions, path constraints and cost functions. Thus, we developed a dedicated model that defines an optimization problem for the closed reference orbit generation. Three terminal boundary constrains on the final position vector in the ITRF2000 reference frame were specified, together with a set of bounds to limit the allowed variation of the initial Keplerian elements. After the optimization, the remaining difference between the initial and the final ITRF position (after one cycle) is typically below 5 mm (3d). The discrepancy in the velocity is below 1

[1] For Sun-synchronous orbits the line of nodes is fixed relative to the Sun implying constant illumination conditions on the spacecraft and on the ground (ground lighting conditions).

[2] For minimum altitude variation or "frozen" orbits[3)] the perturbation of the orbit eccentricity and argument of perigee are minimized yielding nearly equal altitudes in consecutive passes over same ground areas.

[3] Repeat-ground-track orbits provide periodic coverage over same ground locations with identical flight paths. This can only be achieved for draconic or nodal periods which are a rational fraction of a day, e.g. 167/11 days for TSX.

cm/s (3d).

With the new optimization approach we get rid of inconsistencies and nodal period variation stemming from the virtual maneuvers applied in the previous process.[1)] We now obtain a smooth ephemeris being free of state discrepancies within the repeat cycle as well as at the transition to the next cycle.

3. Long-term orbit stability

Unlike the generated reference orbit, the true satellite orbit is exposed to third body and tidal gravitation, irregularities of the earth's rotation and solar radiation pressure (the impact of atmospheric drag will be treated in sect. 5). In order to investigate the impact of the perturbations, the found reference orbit initial state is numerically propagated over one year and the resulting osculating Keplerian elements are monitored w.r.t. the time-mapped reference orbit ephemeris. In the following graphs three integration scenarios are depicted:

- The numerical integration results using exactly the same force model as used in the reference orbit generation process (i.e. earth gravity field with degree 60 and order 60) are depicted as red curves.
- The results for orbit integration considering additionally luni-solar gravitation, solid tides gravitation and irregularities of the earth's rotation are shown as blue curves.
- Finally, the solar radiation pressure (SRP) effect is enabled for the green curves.

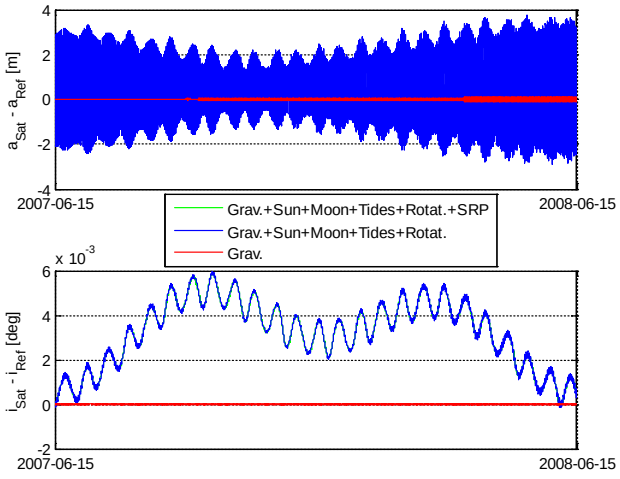

Fig. 2. TSX-Ref relative semi-major axis (top) and relative inclination (bottom).

Disabling all perturbations except for the earth gravity field yields stable Sat-Ref relative orbital elements (cf. red curves in Fig. 2-4). The found small deviations in Δa and Δi result from numerical precision and error propagation over 1-year period. The very small eccentricity vector variation of $a \cdot |\Delta\vec{e}| \cong 1$ m is a well-tolerable left-over from the frozen orbit adjustment step. Finally, the small variations in Δa and Δi build up to a small $\Delta\Omega$. The underlying relation will be explained in sect. 4.

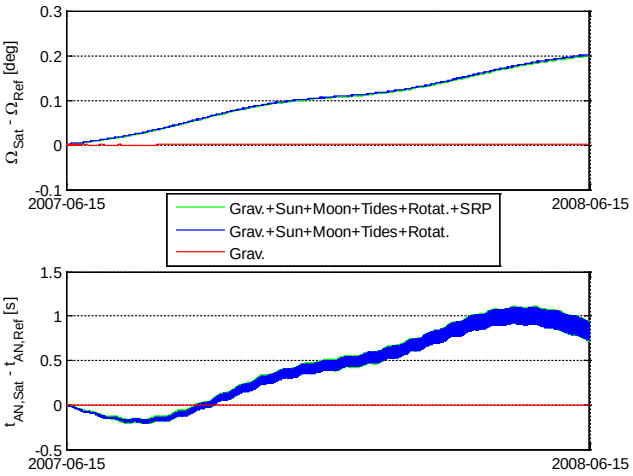

Fig. 3. TSX-Ref relative RAAN (top) and relative ascending node crossing time (bottom).

The third-body gravitation causes secular changes only in the RAAN, the argument of perigee, and the mean anomaly, while periodic changes are induced in the eccentricity, the inclination, the RAAN, and the argument of perigee.[5)] The impact can nicely be seen for Δi (Fig. 2 bottom) and $\Delta\Omega$ (Fig. 3 top). The relative semi-major axis Δa shows periodic variations with the period length being equal to the orbital period.

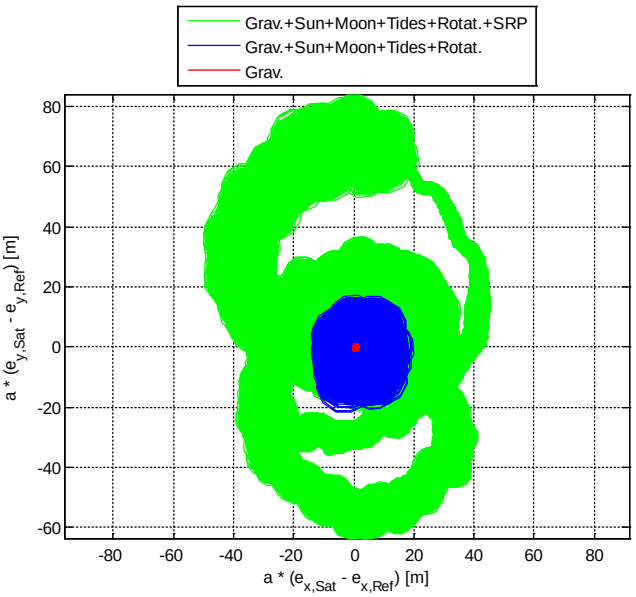

Fig. 4. TSX-Ref relative eccentricity vector $a \cdot \Delta\vec{e}$.

The impact of irregularities of the earth's rotation can be seen as tiny variations in Δa and Δi, which are also present in

ΔΩ but difficult to see in Fig. 3. Finally, the solar radiation pressure (SRP) mainly impacts the eccentricity vector evolution. In Fig. 4 the Sat-Ref relative eccentricity vector is depicted, which follows from the argument of perigee and eccentricity as

$$a\vec{e} = a\begin{pmatrix} e_x \\ e_y \end{pmatrix} = ae\begin{pmatrix} \cos\omega \\ \sin\omega \end{pmatrix}. \quad (1)$$

4. Analysis of inclination sensitivity

The orbit control strategy implemented for TerraSAR-X and foreseen for EnMAP and Tandem-L aims on maintaining the Sat-Ref longitude difference within a control band being equivalent to a distance of ±250 m for TerraSAR-X and Tandem-L and ±22 km for EnMAP. In the following we will focus on the more challenging 250 m requirement, which translates into a ±0.002° ΔΩ band. The variation of ΔΩ is not controlled via expensive RAAN correction maneuvers, but indirectly by drag make-up maneuvers, for details please refer to Ref. 2). As a consequence, the secular RAAN drift of the reference orbit (cf. Fig. 3) has to be compensated too, which leads to a change in the Sat-Ref flight-time difference of $-\Delta\Omega/\omega_E$ with $\omega_E = 2\pi/86400s$ being the Earth's angular velocity.

Therefore, our target for the improved reference orbit process is to minimize the total flight time difference Δt_{Flight} that builds up from differences in the ascending node crossing time (Fig. 3 bottom) and secular changes of the RAAN

$$\Delta t_{Flight} = \Delta t_{AN} - \Delta\Omega/\omega_E. \quad (2)$$

Both terms in Eq. (2) strongly depend on the inclination. The underlying relations will be worked out in the following. The starting points of our analysis are the secular rates of change of the Keplerian elements considering first-order terms in J_2 only as given in Ref. 6)

$$\begin{aligned} \dot{a}_{J_2} &= 0 & \dot{\Omega}_{J_2} &= -\tfrac{3}{2}\beta\cos i \\ \dot{e}_{J_2} &= 0 & \dot{\omega}_{J_2} &= -\tfrac{3}{4}\beta(1-5\cos^2 i) \\ (\dot{i})_{J_2} &= 0 & \dot{M}_{J_2} &= -\tfrac{3}{4}\sqrt{1-e^2}\beta(1-3\cos^2 i) \end{aligned} \quad , \quad (3)$$

where

$$\beta = nJ_2\tfrac{R_E^2}{a^2(1-e^2)^2} \text{ and } n = \sqrt{\mu/a^3} \quad (4)$$

with M being the mean anomaly, n being the mean motion, μ = 398600.4415 km³/s² being the Earth's gravitational parameter, J_2 = 0.00108263 being the geopotential second zonal harmonic, and R_E = 6883.513 km being the Earth's equatorial radius.

From the time-integration of the partial derivation of $\dot{\Omega}_{J_2}$ in Eq. (3) we find for the influence of small inclination changes Δi

$$\Delta\Omega(\Delta i) = \Delta\Omega_0 + \tfrac{3}{2}\beta\sin i\int\Delta i(t)dt. \quad (5)$$

In Fig. 6 we have summed up the found relation in Eq. (5) and the natural RAAN evolution (green curve) with $\Delta i(t)$ being the difference of controlled [4] and uncontrolled inclination (magenta and green curves in Fig. 5). The resulting cyan curve in Fig. 6 matches the ΔΩ found from numerical integration over the inclination control maneuvers (magenta curve) pretty well. A better match might be obtained when considering higher-order terms in J_2, but the achieved accuracy is fully sufficient for our purpose.

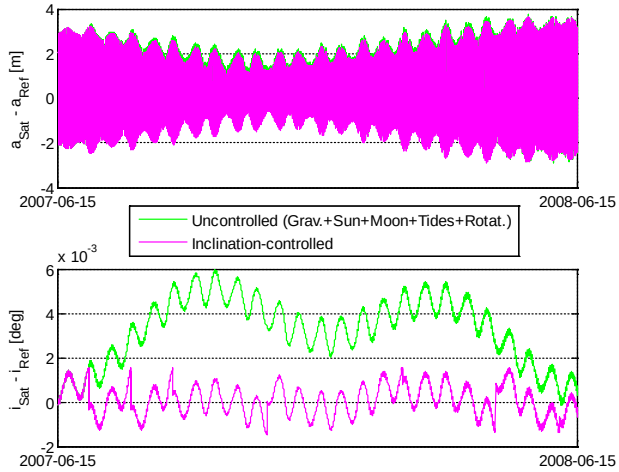

Fig. 5. Natural (green) and inclination-controlled (magenta) evolution of TSX-Ref relative semi-major axis (top) and inclination (bottom).

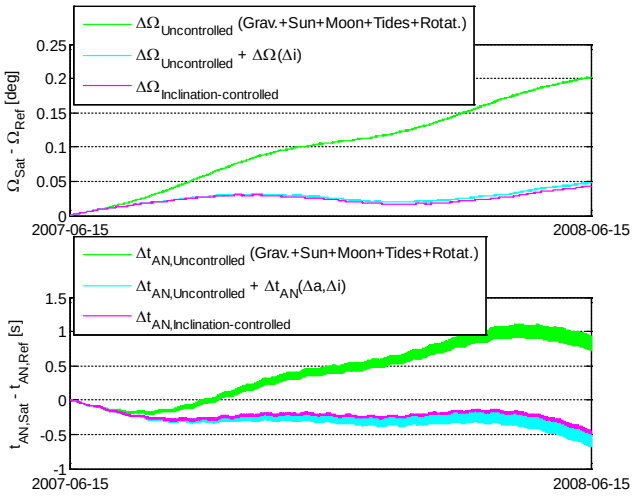

Fig. 6. Natural (green), inclination-controlled (magenta) and modelled (cyan) evolution of TSX-Ref relative RAAN (top) and difference in ascending node crossing time (bottom).

In a similar way we now derive a relation for the change of the ascending node crossing time, which can be expressed as

$$\Delta t_{AN} = \tfrac{1}{n}(\Delta u + \Delta\Omega\cos i) \quad (6)$$

with $\Delta u = \Delta\omega + \Delta M$ being the Sat-Ref difference in mean argument of latitude and $\Delta\Omega\cos i$ being the projection of the Sat-Ref RAAN difference into the flight direction. For Δu we

[4] Inclination maneuvers are modelled in order to maintain the Sat-Ref relative inclination within ±0.0015° while minimizing the yearly Δv.[2)]

have to consider the inclination dependency implied in Eq. (3)

$$\dot{u}_{J_2} = \dot{\omega}_{J_2} + \dot{M}_{J_2} \cong \frac{3}{2}\beta(4\cos^2 i - 1) \quad (7)$$

and the semi-major axis dependency following from the mean motion

$$\dot{u}_a = \sqrt{\mu} a^{-3/2}. \quad (8)$$

Note that to derive the relation in Eq. (7) we simplified $\sqrt{1-e^2} \cong 1$ for e << 1. Inserting $\Delta\Omega_{J2}$ given in Eq. (5) and the time-integration of partial derivatives $\partial\dot{u}_{J2}/\partial i\,\Delta i$ and $\partial\dot{u}_a/\partial a\,\Delta a$ into Eq. (6) yields

$$\Delta t_{AN}(\Delta a, \Delta i) = -\frac{3}{2a}\int \Delta a(t)dt - \frac{21}{4}\frac{\beta}{n}\sin 2i \int \Delta i(t)dt \quad (9)$$

From comparison of numerical (magenta) and modelled (cyan) evolution of Δt_{AN} in Fig. 6 we again find a pretty good match. This implies that the relations derived in Eq. (5) and (9) can be applied to determine the impact of small inclination adjustments to the reference orbit.

5. Inclination adjustment

The changes of $\Delta\Omega$ and Δt_{AN} presented in Fig. 6 for the inclination-controlled scenario translate into a yearly flight-time drift of -10.8 s when using Eq. (2). Note that this is larger than the -8 s observed for the flown TerraSAR-X orbit in year 2013 (Fig. 1). The reason can be found in the different reference orbit used within this study[5] and differences in the underlying relative inclination evolution.

From the results derived in Sect. 4 we draw two conclusions: a) the yearly change of the Sat-Ref flight-time offset is very sensitive to the inclination control strategy, and b) it can be minimized by a proper adjustment of the reference orbit inclination, i.e.

$$min|\Delta t_{AN}(\Delta a, \Delta i) - \Delta\Omega(\Delta i)/\omega_E|. \quad (10)$$

The necessary adjustments are on the order of -0.001°, i.e. -0.00095° for TerraSAR-X, -0.00118° for EnMAP, and -0.00115° for Tandem-L. However, these tiny adjustments cannot directly be applied within the reference orbit process, because the numerical integration of the inclination-corrected initial state no longer fulfills the requirement of matching exactly the same state vector in the Earth-fixed frame after one repeat cycle.

Instead, we apply the small inclination change at every reference orbit ephemeris point that follows from the process described in Sect. 2. The achieved mean reference orbit elements for the three missions are summarized in Tab. 2.

Finally, the tuned reference orbits are validated by means of a 1-year numerical simulation comprising full perturbation model including atmospheric drag, realistic drag make-up and inclination correction orbit control maneuvers. Figure 7 depicts the results obtained for the Tandem-L simulation within a period of moderate solar activity. The Sat-Ref inclination is controlled within a ±0.0015° control band, and drag make-up maneuvers are triggered when $\Delta\Omega_{Sat} - \Delta\Omega_{Ref}$ exceeds +0.002°, which is equivalent to a Sat-Ref displacement of 250 m in normal direction at equator crossings. The tangential maneuver planning aims on maximum maneuver cycles (time from one maneuver to the next) while maintaining $\Delta\Omega_{Sat} - \Delta\Omega_{Ref}$ within ±0.002°.

Table 2. Mean orbital elements of the improved reference orbits.

	TerraSAR-X	EnMAP	Tandem-L
Semi-major axis, km	6883.513	7020.447	7118.619
Eccentricity	0.00125	0.00120	0.00117
Inclination, deg	97.445	97.978	98.377

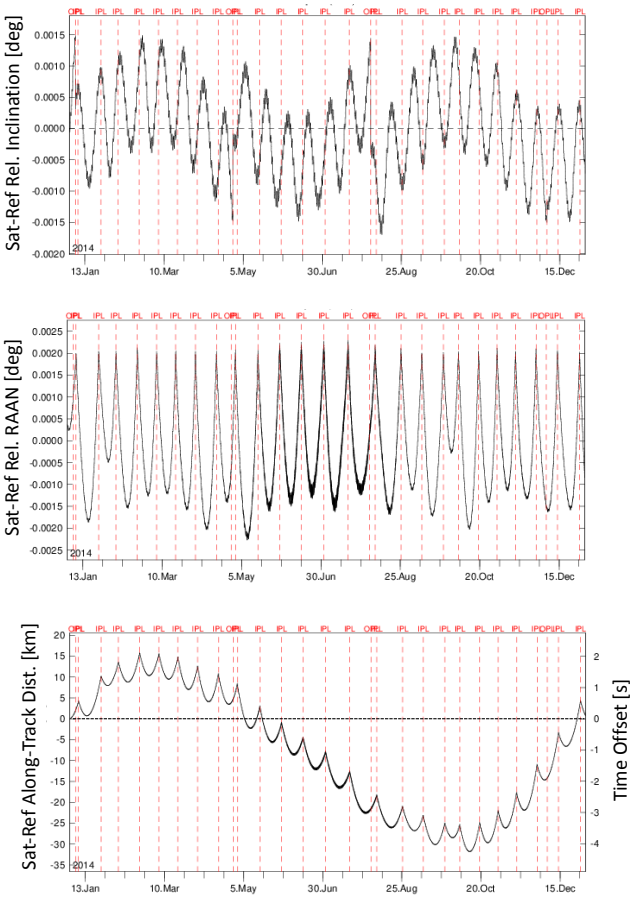

Fig. 7. 1-year simulation of Tandem-L orbit maintenance: Sat-Ref relative inclination (top), RAAN (middle), and along-track distance and corresponding time off-set (bottom). Vertical red lines indicate in-plane (IPL) and out-of-plane (OPL) orbit control maneuvers.

Similar results are obtained for the orbit control simulations of TerraSAR-X and EnMAP. From the found evolution of the time offset in Fig. 7 (bottom) we conclude that the secular time-offset can be eliminated by a small inclination adjustment within the improved reference orbit process. However, the variation within a maneuver cycle and a seasonal variation remain. The magnitude of the variation

[5] The reference orbit implemented for TerraSAR-X operations was created according to the process in Ref. 1) and includes two virtual orbit control maneuvers that influence the nodal period.

depends on the chosen inclination control strategy and is about 5 s for our missions.

6. Conclusion

Our previous process for generation of precise reference orbits[1)] has been reworked and improved in order to eliminate disturbing effects experienced within 10 years of TerraSAR-X operations.

The reference orbit optimization step, which aims on the exact matching of the Earth-fixed states at beginning and end of the repeat cycle, has been changed to optimize the initial state instead of virtual orbit maneuvers, which are no longer needed. We now obtain a smooth ephemeris being free of state discrepancies within the repeat cycle as well as at the transition to the next cycle. The states perfectly match with mm and cm/s accuracy.

From long-term orbit integration including third-body and tidal perturbations as well as inclination correction strategy we determine the inclination adjustment necessary to compensate the secular drift of the Sat-Ref along-track separation. The inclination adjustment is applied at every reference orbit ephemeris point. Finally, a 1-year simulation comprising solar radiation pressure, air drag, inclination correction and drag make-up maneuvers is carried out to proof the stability of the orbit and to validate the refined reference orbit.

Although the inclination adjustment is only about -0.001°, it cannot be applied to the flying TerraSAR-X mission, because it would translate into a lateral ground-track shift larger than 100 m at polar latitudes. However, the reference orbits generated by the improved process discussed in this paper will form the basis for precise orbit control and mission planning of the EnMAP and Tandem-L missions, which are supposed to launch in years 2020 and 2023, respectively.

Acknowledgments

The work described here was carried out as part of the DLR projects TerraSAR-X, EnMAP and Tandem-L.

References

1) D'Amico, S., Arbinger Ch., Kirschner M., Campagnola S.: Generation of an Optimum Target Trajectory for the TerraSAR-X Repeat Observation Satellite, 18th International Symposium on Space Flight Dynamics, Munich, Germany (2004).
2) Kahle, R., D'Amico, S.: The TerraSAR-X Precise Orbit Control – Concept and Flight Results, 24th International Symposium on Space Flight Dynamics, Laurel, Maryland, USA (2014).
3) Rosengren, M.: Improved Technique for Passive Eccentricity Control; AAS Symposium on Mission Design and Orbital Mechanics, AAS 89-155 (1989).
4) GESOP 7 User Manual, Version 7.1.1, Astos Solutions GmbH, 2013.
5) Smith, D. E.: The Perturbation of Satellite Orbits by Extra-Terrestrial Gravitation, *Planet. Space Sci.*, **9** (1962), pp. 659-674.
6) Brouwer, D.: Solution of the problem of artificial satellite theory without drag, *Astronomical Journal*, **64** (1959), pp. 378-396.